

# COMPARING LOAD DISTRIBUTION CALCULATION METHODS IN ROLLING ELEMENT BEARINGS

MÁRIO C. RICCI

National Institute for Space Research (INPE)  
Av. dos Astronautas, 1758, 12227-010 São José dos Campos, Brazil  
e-mail: mario.ricci@inpe.br, [www.inpe.br](http://www.inpe.br)

**Key words:** Rolling Element Bearing, Radial Load, Load Distribution.

**Abstract.** There are two basic methods for radial external load distribution calculation on rolling elements in a rolling element bearing: the discrete method and the integral method. Solving the discrete equilibrium equation using the Newton-Raphson scheme, more accurate results are derived than those based on the integral method, with small theoretical and computational efforts. The Sjövall's radial integral factors, as well as some approximations proposed in the literature, for line- and point-contacts, are given. Numerical approximations for the Sjövall's radial integrals are proposed. The approximations' errors with respect to the Sjövall's radial integral's numerical integration are shown.

## 1 INTRODUCTION

The performance of rolling bearing systems, as well as the life, load capacity, vibration level, noise, running accuracy, stiffness, depend on the geometry of the bearing, including the diametrical clearance, the materials that make up the parts, hardness of contacting surfaces and the load distribution of the external load. This work deals with the external radial load distribution on the rolling elements.

Ref. [1] investigated the load distribution on rolling elements of a radially loaded ball bearing and found that the *maximum* ball load could be obtained by multiplying the *medium* external load by 4.37, for zero internal clearance. This number came to be known as Stribeck's Constant or Number and, to account for nonzero diametrical clearance and other effects, Stribeck recommended rounding the Constant to 5.0.

An integral method for load distribution calculation in bearings was proposed [2]. The relationship between the maximum loaded rolling element load and the bearing external load was established using Sjövall's integrals.

Ref. [3] stated that the theoretical value of Stribeck's Constant for roller bearings with zero internal clearance is 4.08 and suggested using Stribeck's recommended value of 5.0 for the Stribeck's Constant for either ball or roller bearings having typical clearance.

Ref. [4] showed how the Stribeck's Constants were found. It's also shown that the error when adopting the value 4.08 for roller bearing Stribeck's Constant is 55.6 times greater than when adopting the value 4.37 for the ball bearing Stribeck's Constant.

A comprehensive mathematical model of bearings was developed in Ref. [5], which described methods for internal loading distribution in statically loaded bearings addressing pure radial; pure thrust (centric and eccentric loads); combined radial and thrust load, using

radial and thrust Sjövall's integrals' approximations; and for ball bearings under combined radial, thrust, and moment load. The load zone was described by the load distribution factor,  $\epsilon$ , and the contact stress-strain relationship between the ring and any rolling element was achieved. The load distribution can be obtained by continuous iteration procedure. However, studies have shown [6, 7] that the results obtained by the Harris method [5] can't rigorously satisfy the static balance. Pointing out that the problem of obtaining the load distribution in bearings with arbitrary radial clearance is to determine the number of rolling elements that participate in the transfer of the external radial load.

A new approach in the mathematical modeling of rolling bearings was developed [6-8]. The approach considers two boundary cases of inner ring support on an even and/or odd number of rolling elements. In relation to these boundary conditions, Tomović derived the general equations for the calculation of the boundary deflection and internal radial load values, which are necessary for the inner ring support on a finite number of rolling elements.

The effect of internal clearance on load distribution and fatigue life of radially loaded deep groove ball bearings was investigated [9, 10]. They found that life gradually decreases with increasing clearance's absolute value and is maximum under small negative clearance. Furthermore, in radially loaded bearings, the rolling elements, which transfer the load – active elements –, are located below the meridian plane in the so-called *loading zone*. The quasi-static analysis to derive the radial load distribution is based on the assumption that the inner ring, under load, moves radially in the direction of the external load, with respect to the outer ring, which rings are considered rigid.

There are two basic methods for radial external load distribution determination on rolling elements, which participate in the load transfer between rings in a rolling element bearing. There is a *discrete method*, where the radial external load, the diametrical clearance, the load-deflection relationships at the rolling elements-race contacts are known and assuming that the rolling elements are symmetrically and evenly distributed with respect to the radial external load direction, the rolling elements normal loads, the relative radial displacement between rings or the deflection at maximum loaded rolling element can be obtained by numerically satisfying the static equilibrium equation, which requires that the applied load must be equal to the sum of the rolling elements loads components parallel to the direction of the applied load.

There is a second method - *integral method* -, where the rolling element normal load equivalent to a rolling element-race elastic hertzian contact deflection equal to the relative displacement between the rings can be given by multiplying the reciprocal of an *integral* factor and the applied external radial load *averaged*. Equivalently, the maximum rolling element normal load of the bearing can be given by multiplying the reciprocal of a second integral factor and the applied external radial load averaged.

The integral methods described in the literature for normal rolling elements load distribution in a rolling bearing under radial external load require the integration, around the load zone, of a trigonometric function, which the cosine of the loading zone azimuth angle is the parameter – the Sjövall radial integral. This integral can be reduced to a standard elliptical integral by the hypergeometric series and the beta function, requiring reasonable theoretical effort. In applications, a numerical evaluation of the integral is used, therefore, an approximation of the exact solution.

The method described in this work obtain numerically the *shift* between rings – or the maximum elastic hertzian deflection at race-rolling element contacts - and, therefore, the normal rolling elements loads, using *a single* iterative numerical based Newton-Raphson equation; and it was found that the method described in this work obtain results as accurate as, or even more accurate than the methods described in the literature, with little theoretical and computational effort. Then, in this work is described a simple, accurate numerical iterative Newton-Raphson based method for internal load distribution computation in statically loaded, single-row, deep groove, angular-contact ball bearings or cylindrical roller bearings, subjected to a known external radial load. The author didn't find in the literature the resolution of this problem using the procedure here described.

Many of the introductory subjects have already been addressed in other papers by other authors and aren't repeated here (geometry of ball and roller bearings, formulas for normal stresses and deflections calculations when two elastic solids are brought into contact, relationships between load and deflection for static loading). Symbols used in formulas are introduced as they appear in the text. The formulas for static loading of ball and roller bearings are presented, including equilibrium equations in the discrete and integral forms. The former presented as a sum of the normal rolling element loads components in the direction of the external load, and the last as an integral around the loading zone.

The two Sjövall's radial integral factors, relating the maximum loaded rolling element load and the average external load, are given, as well as approximations for radial integrals due to [9-11], for line- and point-contacts. The approximations' errors with respect to the Sjövall's radial integral's numerical integration are shown. A numerical approximation for the Sjövall's radial integral is proposed, which fits the numerical integration properly for almost the entire load zone range, for both, line- and point-contact, which has shown to have smaller errors than other approximations for small load zones.

In sequence, one iterative scalar equation for the radial total displacement between the rings using the Newton-Raphson method is introduced. Knowing the radial total displacement or the maximum deflection and the diametrical clearance, the other parameters can be found, for both ball and roller bearings: the distance between shifted groove curvature centers - considering that for this type of loading, the all balls contact angles are null; the normal load, maximum deflection and contact ellipse parameters for each ball of the ball bearing; maximum deflection and semiwidth contact parameters for each roller of the roller bearing. Numerical results of the presented Newton-Raphson based method are shown through plots, for 209, 210 and 218 deep groove or angular-contact ball bearings, and have been compared with Stribeck's results, which consider *null* diametrical clearance for a complete range of the radial load; with an approximate iterative integration method described in Ref. [11], with results shown in Refs. [9, 10], and with approximations suggested in this work.

## 2 ROLLING ELEMENT BEARINGS UNDER RADIAL LOAD

Let a bearing with  $Z$  rolling elements (balls or rollers) symmetrically distributed about a pitch circle to be subjected to a radial load. Then, a *relative radial displacement*,  $\delta$ , between the inner and outer ring raceways may be expected. Let  $\psi$  the azimuth angle measured from the load line, which passes through the most loaded element (Fig. 1).

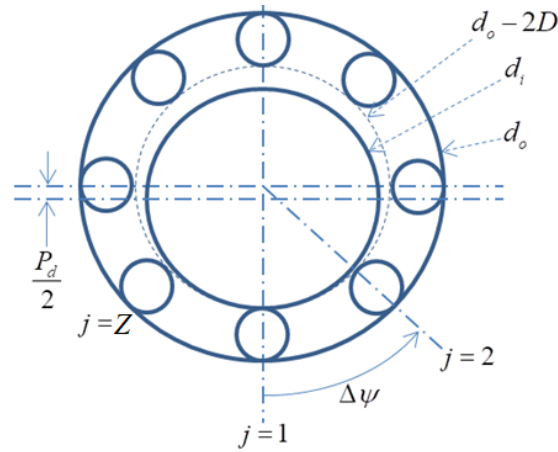


**Figure 1:** Rolling elements angular positions in the radial plane, which is perpendicular to the bearing's axis of rotation,  $\Delta\psi = 2\pi/Z$ ,  $\psi_j = \Delta\psi(j-1)$ ,  $j = 1, \dots, Z$ ;  $P_d$  represents the diametrical clearance;  $d_o$ ,  $d_i$ ,  $D$  represent outer, inner raceway diameters, and rolling element diameter, respectively

The original diametrical clearance, as a result of the bearing manufacturing process, may change after fitting and under temperature's radial gradients between rings and rolling elements, when in operation; and may result in clearance or interference (preloading). Therefore, I assume here that the resulting operational diametrical clearance can be positive, negative or zero.

A loaded radially bearing with diametrical clearance  $P_d > 0$ , at which the load line passes through the most loaded rolling element's center is shown in Fig. 2. In the concentric position shown in Fig. 2(a), a uniform radial clearance of  $P_d/2$  is observed between the rolling elements and the raceways. The application of a small radial load to the shaft causes the inner ring to move a distance  $P_d/2$  before contact between the rolling element located on the load line at  $\psi = 0$  and the inner and outer raceways.

However, if  $P_d < 0$  in the concentric position, a uniform radial *preload* is observed and the application of a small radial load to the shaft causes the inner ring to move a distance  $|P_d|/2$  before release of the rolling element located on the load line at  $\psi = 180^\circ$  from the inner and outer raceways.

The radial clearance or interference,  $c_j$ , at a given azimuth angle  $\psi_j$ , if  $|P_d|$  is small compared to the radius of the tracks, can be expressed with adequate precision by

$$c_j = \left( 1 - \frac{|P_d|}{P_d} \cos \psi_j \right) \frac{P_d}{2}. \quad (1)$$

Note that Eq. (1) introduced in this work is slightly different from the equation proposed for the clearance on p. 21 of the Ref. [11], which is assumed positive. Eq. (1) allows working with the clearance sign easily. If  $P_d > 0$ , on the load line where  $\psi = \psi_1 = 0^\circ$ , the clearance is zero; but when  $\psi = 180^\circ$  the clearance is  $P_d$ . If  $P_d < 0$  the clearance is null at  $\psi = 180^\circ$  and  $P_d$  (interference) at  $\psi = 0^\circ$ .

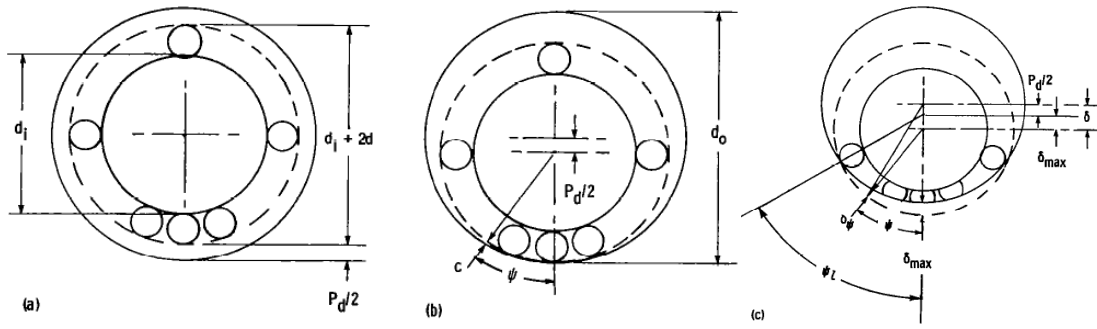


**Figure 2:** Radially loaded bearing with diametrical clearance  $P_d > 0$ , at which the load line passes through the most loaded rolling element's center: (a) Concentric arrangement; (b) Initial contact; (c) Interference  
Source: [11]

The application of further load will cause elastic deformation of the rolling elements along a  $2\psi_l$  arc. If the further elastic interference or compression in the load line is  $\delta_{\max}$  the corresponding elastic compression  $\delta_j$  of the rolling element along a radius at an angle  $\psi_j$  to the load line is given by

$$\delta_j = \delta_{\max} \cos \psi_j - c_j, \quad (2)$$

which assumes that the rings are rigid.

Substituting (1) in (2), yields

$$\delta_j = \delta \cos \psi_j - \frac{P_d}{2}, \quad (3)$$

where

$$\delta \triangleq \delta_{\max} + \frac{|P_d|}{2} \quad (4)$$

represents the *total relative radial displacement* between inner and outer rings.

Substituting (3) in the load-deflection relationship, yields

$$Q_j = K_n \left( \delta \cos \psi_j - \frac{P_d}{2} \right)^n, \quad (5)$$

where  $Q_j$  is the normal load of the rolling element along a radius at an angle  $\psi_j$  to the load line,  $K$  is the load-deflection factor and  $n$  is the load-deflection exponent.

For static equilibrium, the applied load  $F_r$  must be equal the sum of the components of the rolling-elements loads parallel to the direction of the applied load, that is,

$$F_r = \sum_{j=1}^Z Q_j \cos \psi_j. \quad (6)$$

Substituting (5) in (6), yields

$$F_r = K_n \sum_{j=1}^Z \left( \delta \cos \psi_j - \frac{P_d}{2} \right)^n \cos \psi_j, \quad (7)$$

in which are not all rolling elements that work, but those in the angular extension of the bearing arc  $2\psi_l$ , in which the rolling elements are loaded. This load zone is obtained by setting the expression between curved brackets in (5) equal to zero and solving for  $\psi$ , yields

$$\psi_l = \cos^{-1} \left( \frac{P_d}{2\delta} \right). \quad (8)$$

Therefore, (7) can be written in the integral form by

$$F_r = ZK_n \delta^n J_r'(\psi_l), \quad (9)$$

where

$$J_r'(\psi_l) \triangleq \frac{1}{2\pi} \int_{-\psi_l}^{\psi_l} (\cos \psi - \cos \psi_l)^n \cos \psi d\psi \quad (10)$$

is known as the Sjövall's radial integral.

Defining the load distribution factor,

$$\varepsilon \triangleq \frac{1}{2}(1 - \cos \psi_l), \quad (11)$$

as being the ratio between the load zone projected on line load bearing diameter and the diameter, then (9) can be written by

$$F_r = ZQ_{\max} J_r(\varepsilon), \quad (12)$$

where

$$J_r(\varepsilon) \triangleq \frac{1}{2\pi} \int_{-\psi_l}^{\psi_l} \left[ 1 - \frac{1}{2\varepsilon}(1 - \cos \psi) \right]^n \cos \psi d\psi. \quad (13)$$

Since  $n$  is a fractional power in the Eqs. (10) and (13), then these equations can be reduced to standard elliptical integrals by hypergeometric series and beta function [11].

The load carried by the most heavily loaded rolling element is obtained by substituting  $\psi_{j=1} = 0^\circ$  in Eq. (7), dropping the summation sign, yields

$$Q_{\max} = K_n \delta^n (1 - \cos \psi_l)^n = K_n \delta^n (2\varepsilon)^n, \quad (14)$$

which substituted in Eq. (12) shows that the integral in Eq. (13), when multiplied by the factor between curved brackets raised to the power  $n$  of the Eq. (14), results the integral in Eq. (10).

For *roller bearings*  $n = 10/9$ , but if  $n$  is approached by 1, the integrals (10) and (13) can be approximate by [11]

$$J_r'(\psi_l) \cong \frac{1}{2\pi} (\psi_l - \cos \psi_l \sin \psi_l) \quad (15)$$

and

$$J_r(\varepsilon) \cong \frac{1}{4\pi\varepsilon} \left[ \cos^{-1}(1 - 2\varepsilon) - (1 - 2\varepsilon) \sqrt{1 - (1 - 2\varepsilon)^2} \right]. \quad (16)$$

The following fitting for the numerical evaluation of Eq. (13),

$$J_r \cong 0.3268\varepsilon^{0.4023}, \quad 0 \leq \varepsilon < 0.5, \quad (17)$$

$$J_r \cong 0.2451, \quad \varepsilon = 0.5, \quad (18)$$

$$J_r \cong -0.0852\varepsilon^4 + 0.5703\varepsilon^3 - 1.3343\varepsilon^2 + 1.775\varepsilon - 0.0771, \quad 0.5 < \varepsilon \leq 2, \quad (19)$$

was proposed in Refs. [9, 10] for a line contact. However, the proposed fitting for  $0.5 < \varepsilon \leq 2$  is inadequate, and, therefore, I propose the following fitting

$$J_r \cong -13.2288\varepsilon^4 + 15.2846\varepsilon^3 - 6.5712\varepsilon^2 + 1.5386\varepsilon + 0.0268, \quad 0 \leq \varepsilon < 0.5, \quad (20)$$

$$J_r \cong 0.2448, \quad \varepsilon = 0.5, \quad (21)$$

$$J_r \cong -0.1070\varepsilon^4 + 0.6773\varepsilon^3 - 1.5169\varepsilon^2 + 1.3025\varepsilon - 0.1082, \quad 0.5 < \varepsilon \leq 2, \quad (22)$$

which best fits the results obtained numerically from the numerical integration of Eqs. (13) and (10), for  $n = 10/9$ , when the imaginary part is disregarded, as shown in Figs. 3(a) and 4(a).

For *ball bearings*  $n = 3/2$ , and the following fitting

$$J'_r(\psi_l) \cong \frac{2.491}{\pi} \left\{ \left[ 1 + \left( \frac{\cos \psi_l - 1}{1.23} \right)^2 \right]^{1/2} - 1 \right\} = \frac{2.491}{\pi} \left\{ \left[ 1 + \left( \frac{2\varepsilon}{1.23} \right)^2 \right]^{1/2} - 1 \right\}, \quad (23)$$

was proposed in Ref. [11] for the Eq. (10) evaluated numerically.

The following fitting for the numerical evaluation of Eq. (13),

$$J_r \cong 0.3076\varepsilon^{0.4175}, \quad 0 \leq \varepsilon < 0.5, \quad (24)$$

$$J_r \cong 0.229, \quad \varepsilon = 0.5, \quad (25)$$

$$J_r \cong -0.0191\varepsilon^4 + 0.202\varepsilon^3 - 0.6327\varepsilon^2 + 0.6805\varepsilon + 0.0213, \quad 0.5 < \varepsilon \leq 2, \quad (26)$$

was proposed in Refs. [9, 10] for a point contact.

I propose the following fitting

$$J_r \cong -12.0191\varepsilon^4 + 13.8882\varepsilon^3 - 5.9563\varepsilon^2 + 1.4033\varepsilon + 0.0244, \quad 0 \leq \varepsilon < 0.5, \quad (27)$$

$$J_r \cong 0.2288, \quad \varepsilon = 0.5, \quad (28)$$

$$J_r \cong -0.0446\varepsilon^4 + 0.3368\varepsilon^3 - 0.8843\varepsilon^2 + 0.8757\varepsilon - 0.0318, \quad 0.5 < \varepsilon \leq 2, \quad (29)$$

which has a similar precision to the Refs. [9, 10] approximation, as shown in Figs. 3(b) and 4(b), but with a slightly wider application range. The Ref. [11] approximation turns out to be more accurate than the Refs. [9, 10] and Ricci's approximations and fits the exact numerical solution to within  $\pm 2$  percent for a complete range of application.

The Fig. 3(a) shows the integral of Eq. (13) calculated numerically for  $n = 10/9$ , the Ref. [11] approx. for  $n = 1$  (Eq. (16)), the Refs. [9, 10] approx. (Eqs. (17)-(19)), and the Ricci's approx. (Eqs. (20)-(22)); conjointly with the relative errors of the approximations with respect to the numerical integration, as functions of  $\varepsilon$ , for  $0 \leq \varepsilon \leq 2$ .

The Fig. 3(b) shows the integral of Eq. (13) calculated numerically for  $n = 3/2$ , the Ref. [11] approx. (Eq. (23)) multiplied by the factor  $(2\varepsilon)^{-3/2}$ , the Refs. [9, 10] approx. (Eqs. (24)-

(26)), and the Ricci's approximation (Eqs. (27)-(29)), together with the approximations' errors with relation to the numerical integration, as functions of  $\varepsilon$ , for  $0 \leq \varepsilon \leq 2$ . Note that the Ref. [11] approx. fits properly only in the range  $0 \leq \varepsilon \leq 1$ .

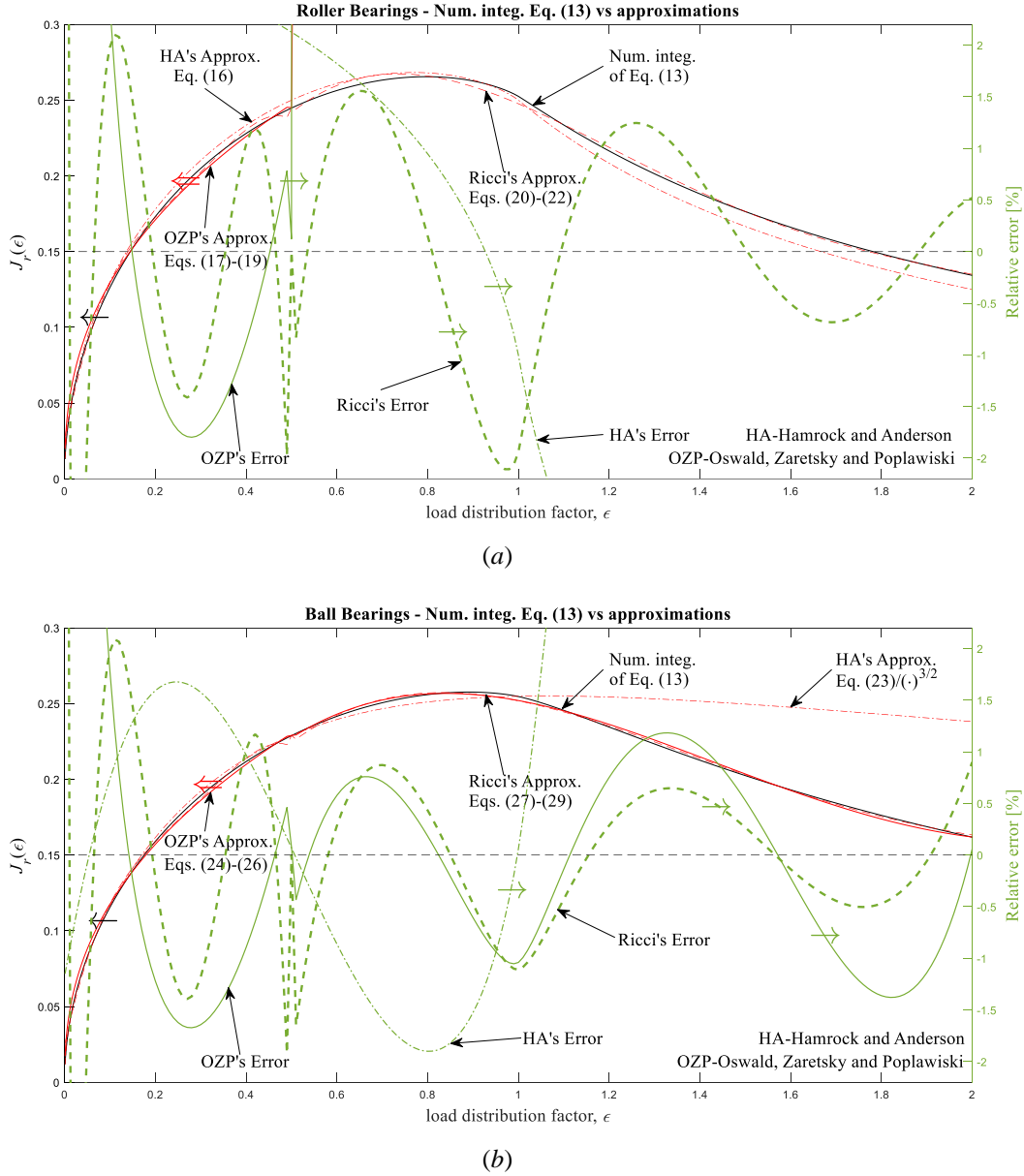


**Figure 3:** Numerical integration of Eq. (13), approximations and relative errors with respect to the numerical integration, as functions of  $\varepsilon$ , for  $0 \leq \varepsilon \leq 2$ . (a)  $n = 10/9$ ; HA's approx. for  $n = 1$  (Eq. (16)); OZP's approx. (Eqs. (17)-(19)); Ricci's approx. (Eqs. (20)-(22)). (b)  $n = 3/2$ ; HA's approx. (Eq. (23)) multiplied by the factor  $(2\varepsilon)^{-3/2}$ ; OZP's approx. (Eqs. (24)-(26)); Ricci's approx. (Eqs. (27)-(29)). HA-Hamrock and Anderson; OZP-Oswald, Zaretsky and Poplawski

The Fig. 4(a) shows the integral of Eq. (10) calculated numerically for  $n = 10/9$ , the Ref. [11] approximation for  $n = 1$  (Eq. (15)), the Refs. [9, 10] proposed fitting (Eqs. (17)-(19)), and

the the Ricci's approx. in Eqs. (20)-(22), with last two approximations multiplied by the factor between curved brackets raised to the power  $n = 10/9$  in the Eq. (14). In addition, the Fig. 4(a) shows the relative errors of the approximations with respect to the numerical integration, as functions of  $\psi_l$ , for  $0^\circ \leq \psi_l \leq 180^\circ$ .

The Fig. 4(b) shows the integral of Eq. (10) calculated numerically for  $n = 3/2$ , the Ref. [11] approximation (Eq. (23)), the Refs. [9, 10] approximation (Eqs. (24)-(26)), and the Ricci's approximation (Eqs. (27)-(29)), with last two approximations multiplied by the factor between curved brackets raised to the power  $n = 3/2$  in the Eq. (14); together with the approximations relative errors with respect to the numerical integration, as functions of  $\psi_l$ , for  $0^\circ \leq \psi_l \leq 180^\circ$ .

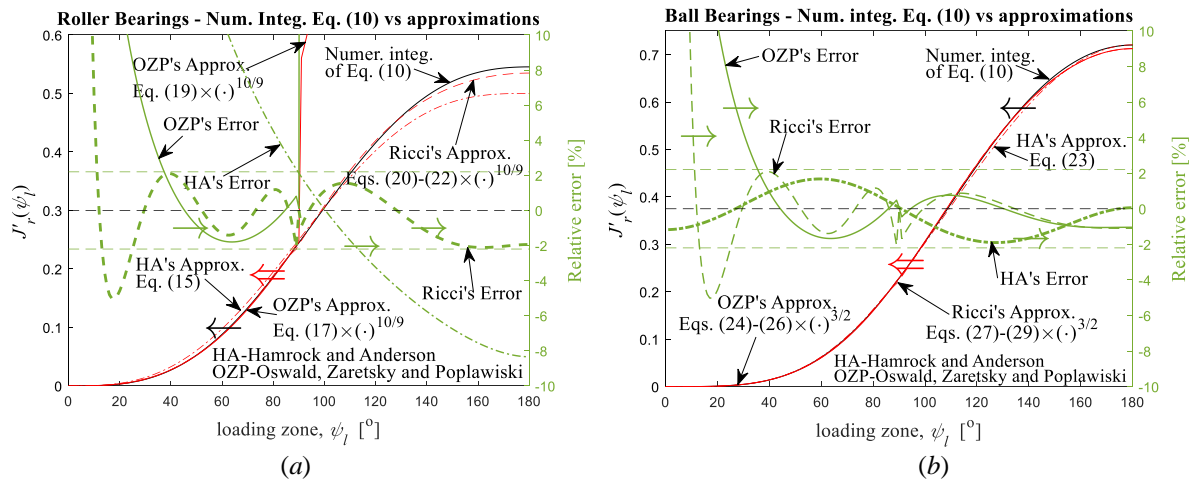


**Figure 4:** Numerical integration of Eq. (10), approximations and relative errors with respect to the numerical integration, as functions of  $\psi_l$ , for  $0 \leq \psi_l \leq 180^\circ$ . (a)  $n = 10/9$ ; HA's approx. for  $n = 1$  (Eq. (15)); OZP's approx. (Eqs. (17)-(19)) Ricci's approx. (Eqs. (20)-(22)), with last two approximations multiplied by the factor between curved brackets raised to the power  $n = 10/9$  in the Eq. (14); (b)  $n = 3/2$ ; HA's approx. (Eq. (23)); OZP's approx. (Eqs. (24)-(26)); Ricci's approx. (Eqs. (27)-(29)), with last two approximations multiplied by the factor between curved brackets raised to the power  $n = 3/2$  in the Eq. (14). HA-Hamrock and Anderson; OZP-Oswald, Zaretsky and Poplawski

Replacing Eq. (14) in Eq. (9) and from Eq. (12), yields

$$Q_{\max} = \frac{(1 - \cos \psi_l)^n}{J_r(\psi_l)} \frac{F_r}{Z} = \frac{(2\varepsilon)^n}{J_r(\psi_l)} \frac{F_r}{Z} = \frac{1}{J_r(\varepsilon)} \frac{F_r}{Z}, \quad (30)$$

which represent the ratios between the maximum rolling element's radial load,  $Q_{\max}$ , and the medium or average radial external load,  $F_r/Z$ . The factors multiplying the average radial external load are defined as the Stribeck's Coefficients,  $S_t$ , for ball and roller bearings and differ from Stribeck's Constants or Numbers, which are approximations for Stribeck's Coefficients for a rolling element bearing with zero radial clearance [4, 12].

For  $n = 3/2$ , replacing Eq. (23), in Eq. (30), yields

$$Q_{\max} = \mathcal{Z} \frac{F_r}{Z}, \quad (31)$$

where

$$Z \triangleq \frac{\pi(1 - \cos \psi_l)^{3/2}}{2.491 \left\{ \left[ 1 + \left( \frac{\cos \psi_l - 1}{1.23} \right)^2 \right]^{1/2} - 1 \right\}} = \frac{\pi(2\varepsilon)^{3/2}}{2.491 \left\{ \left[ 1 + \left( \frac{2\varepsilon}{1.23} \right)^2 \right]^{1/2} - 1 \right\}}, \quad (32)$$

is a Stribeck's Coefficients factor approximation for ball bearings.

When the diametrical clearance  $P_d$  is zero, from Eq. (8),  $\psi_l = \pi/2$ , and from Eqs. (30) and (10)

$$Q_{\max} = \frac{1}{J_r(\pi/2)} \frac{F_r}{Z} = 4.37 \frac{F_r}{Z}. \quad (33)$$

Stribeck [1] obtained  $Z = 4.37$ . He then derived the famous Stribeck equation for static load capacity, writing a more conservative value of 5, for take account the diametrical clearance, for the theoretical value of 4.37, that is,

$$F_r = \frac{Z}{5} Q_{\max}. \quad (34)$$

Nowadays, digital computers are quite widespread and hence it is not necessary to calculate radial integrals or to obtain approximations as proposed by Stribeck, Sjövall, Palmgren, Harris, Hamrock and Anderson or Oswald, Zaretsky and Poplawski to obtain the load distribution in a bearing under radial load. This can be achieved easily using a single iterative scalar equation for  $\delta$  or  $\delta_{\max}$ . Given  $F_r$ ,  $K_n$ ,  $P_d$ , and  $\psi_j$ ,  $j = 1, \dots, Z$ , Eq. (7) can be solved numerically for  $\delta$  by the Newton-Raphson method. The iterative equation to be satisfied is

$$\delta_{i+1} = \delta_i + \frac{F_r - \sum_{j=1}^Z K_{nj} \left( \delta_i \cos \psi_j - \frac{P_d}{2} \right)^n \cos \psi_j}{n \sum_{j=1}^Z K_{nj} \left( \delta_i \cos \psi_j - \frac{P_d}{2} \right)^{n-1} \cos^2 \psi_j}, \quad (35)$$

in which the convergence is satisfied when  $\delta_{i+1} - \delta_i$  becomes essentially zero. Having obtained  $\delta$  the normal ball load is easily obtained by Eq. (6).

### 3 NUMERICAL RESULTS

Chosen a rolling bearing, as input, geometric parameters:  $d_i$ ,  $d_o$  - or  $d_a$ ,  $d_b$  -  $D$ ,  $Z$ , and  $f$ ; and elastic properties:  $E_a$ ,  $E_b$ ,  $\nu_a$  and  $\nu_b$ , must be given. Next, the following parameters must be derived:  $d_e$ ,  $\psi_j$ ,  $j = 1, \dots, Z$ ,  $E'$  and  $P_d$ .

The interest here is to observe the behavior of a deep groove, angular-contact ball bearing, under radial load. With the purpose of comparing the numerical results of the Newton-Raphson algorithm based method, developed in this work, with those of the literature, the values  $1/R|_i$ ,  $1/R|_o$ ,  $\Gamma_i$ ,  $\Gamma_o$ ,  $k_i$ ,  $k_o$ ,  $\mathbf{K}_i$ ,  $\mathbf{K}_o$ ,  $\mathbf{E}_i$ ,  $\mathbf{E}_o$ ,  $K_i$ ,  $K_o$  and  $K_n$ , which are functions of the contact angle, are calculated [5]. Since the contact angles are null for this type of loading, these values are constants for all balls angular positions. Initially was given  $\delta$  estimates for

each external radial load varying from zero up to 10,000 N. The news  $\delta$  values are compared with old ones and if relative errors are greater than a minimal error, new  $\delta$  values are derived. If relative errors are lesser than the minimal error, the program ends.

To show an application of the theory developed in this work numerical examples are presented here. I have chosen the 209, 210, and 218 deep groove or angular-contact ball bearings, which were also used in Refs. [5, 9, 10, 11]. Thus, the results obtained here can be compared to a certain degree with the results of the authors' papers cited. The input data for these rolling bearings are shown in Table I.

**Table I:** Input data for ball bearings used as examples

	<b>209</b>	<b>210</b>	<b>218</b>
Bore diameter, $d_b$ [m]	0.045	0.05	0.09
Outer diameter, $d_a$ [m]	0.085	0.09	0.16
Pitch diameter, $d_e$ [m]	0.065	0.07	0.125
Race conformity, $f$	0.52	0.52	0.5232
Ball diameter, $D$ [m]	0.0127		0.02223
Number of balls, $Z$	9	10	16
Modulus of elasticity for both balls and races, $E$ [N/m <sup>2</sup> ]	$2 \times 10^{11}$	$2.059 \times 10^{11}$	$2.075 \times 10^{11}$
Poisson's ratio for both balls and races, $\nu$	0.3		

The Fig. 5 shows the relative total rings radial displacements computed using the Eq. (35) and the approximations of Stribeck [1], Hamrock and Anderson [11], Oswald, Zaretsky and Poplawski [9, 10], and Ricci, as radial external load functions, ranging from zero to 10,000 N, for the 209, 210 and 218 ball bearings. Since the Stribeck's method applies to bearings with zero radial clearance, the nominal radial clearances were added to the Stribeck's results, for the entire radial external load range. Then, the results using Stribeck, Hamrock and Anderson, Oswald, Zaretsky and Poplawski, and Ricci's approximations can be compared with the result of Eq. (35). The dashed lines represent the relative errors of the approximations with respect to the discrete method solved using the Newton-Raphson technique. In the plots of Fig. 5 the ordinate on the left side represents the values of the total radial displacement between the rings derived by all methods and the ordinate on the right side represents the errors, in percentage, of the values of the total radial displacement between the rings obtained by the approximate methods in relation to the obtained by solving Eq. (35).

#### 4 CONCLUSIONS

It has been shown that it is possible to easily and accurately obtain the radial external load distribution applied to a rolling element bearing by solving the quasi-static equilibrium discrete scalar equation using the Newton-Raphson scheme. Approximate methods based on Sjövall integrals - as functions of the load zone or load factor - were compared with the discrete method Newton-Raphson solution and the errors were quantified as a function of the loading. An approximate method was proposed that fits the solutions of the numerical solutions of the Sjövall integrals within a range of  $\pm 2\%$ , which has shown to have better performance than other approximations for small load zones, as shown in Fig. 5(c).

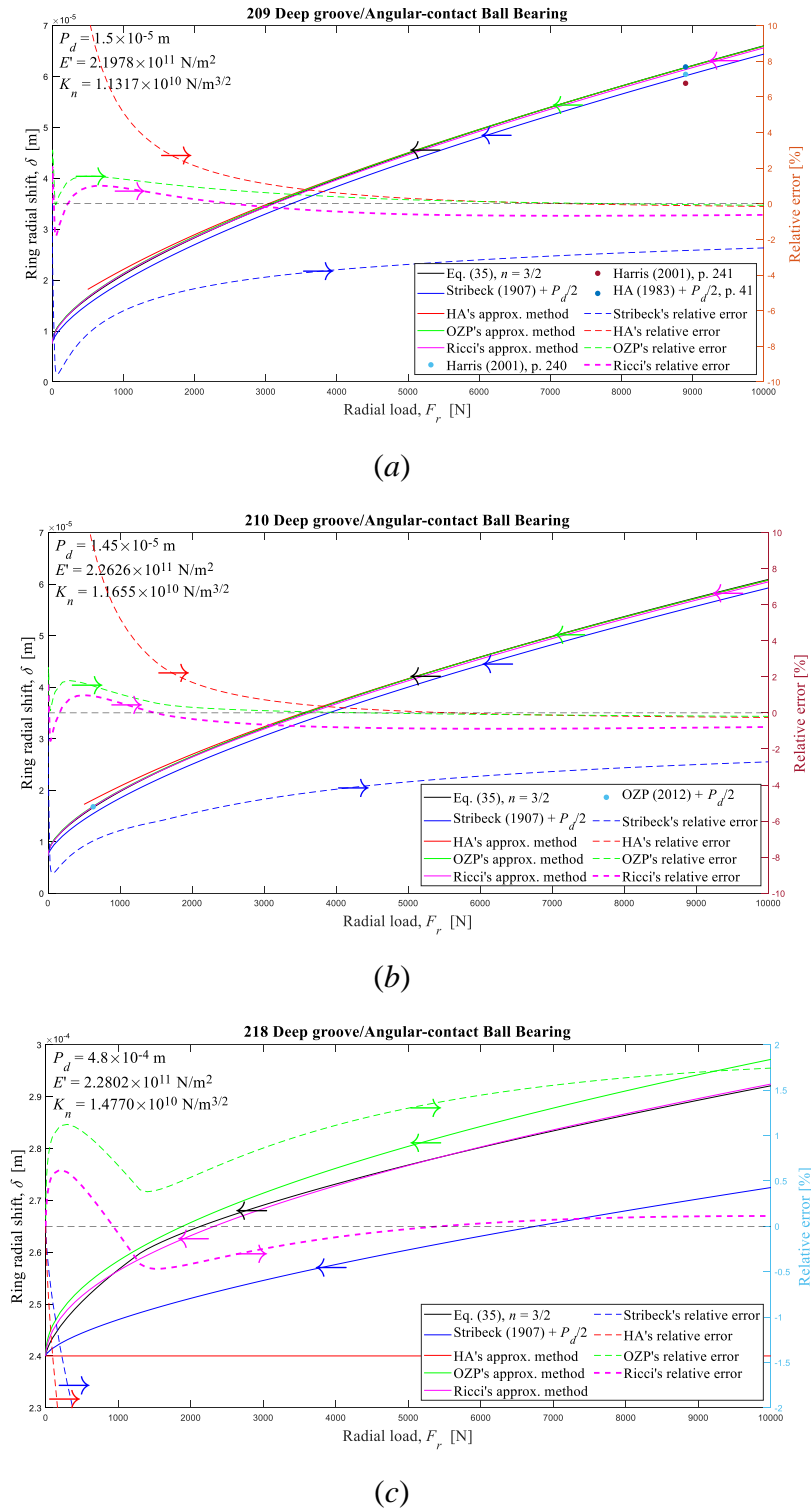


**Figure 5:** Displacement between rigid rings of the deep-groove or angular-contact ball bearing, as a function of external radial load, for five different methods. Results presented in the literature also are shown: (a) 209,  $0.12 < \varepsilon < 0.44$ ,  $41.4 < \psi_l < 83.37^\circ$ ; (b) 210,  $0.14 < \varepsilon < 0.44$ ,  $43.53 < \psi_l < 83.06^\circ$ ; (c) 218,  $0 < \varepsilon < 0.09$ ,  $0 < \psi_l < 34.14^\circ$ . HA-Hamrock and Anderson; OZP-Oswald, Zaretsky and Poplawski

## 5 ACKNOWLEDGMENTS

The author thanks the collaboration of the following institutions: National Council for Scientific and Technological Development (CNPq); Coordination for the Improvement of Higher Education Personnel (CAPES); Research Support Foundation of the State of São Paulo (FAPESP); Ministry of Science, Technology and Innovation (MCTI); National Institute for Space Research (INPE).

## 6 RESPONSIBILITY FOR INFORMATION

The author is solely responsible for the information included in this work.

## REFERENCES

- [1] Stribeck, R. Ball Bearings for Various Loads. *Trans. ASME* (1907) **29**:420-463.
- [2] Sjövall, H. The Load Distribution within Ball and Roller Bearings under Given External Radial and Axial Load. *Teknisk Tidskrift, Mek* (1933), h.9.
- [3] Palmgren, A. *Ball and Roller Bearing Engineering*. 3<sup>rd</sup> ed., Burbank, Philadelphia, (1959).
- [4] Ricci M. C. On the Stribeck's numbers in radially loaded rolling element bearings. *Proceedings CREEM2022* (2022). <https://abcm.org.br/proceedings/view/CRE2022/0038>
- [5] Harris, T. A. *Rolling Bearing Analysis*. 4<sup>th</sup> ed., John Willey & Sons Inc., New York, (2001).
- [6] Tomović, R. Calculation of the boundary values of rolling bearing deflection in relation to the number of active rolling elements. *Mechanism and Machine Theory* (2012) **47**:74-88.
- [7] Tomović, R. Calculation of the necessary level of external radial load for inner ring support on  $q$  rolling elements in a radial bearing with internal radial clearance. *International Journal of Mechanical Science* (2012) **60**:23-33.
- [8] Tomović, R., Miltenović, V., Banić, M. and Miltenović, A. Vibration response of rigid rotor in unloaded rolling element bearing. *International Journal of Mechanical Sciences* (2010) **52**(9):1176-1185.
- [9] Oswald, F. B., Zaretsky, E. V. and Poplawski, J. V. *Effect of Internal Clearance on Load Distribution and Life of Radially Loaded Ball and Roller Bearings*. NASA/TM-2012-217115, (2012).
- [10] Oswald, F. B., Zaretsky, E. V. and Poplawski, J. V. Effect of Internal Clearance on Load Distribution and Life of Radially Loaded Ball and Roller Bearings. *Tribology Transactions* (2012) **55**(2):245–265.
- [11] Hamrock, B. J. and Anderson, W. J., *Rolling-Element Bearings*. NASA RP 1105, (1983).
- [12] Ricci M. C., On load distribution factors in radially loaded rolling element bearings, to be published, (2022).